

Microstructure and Crystallization of Melt-Mixed Poly(ethylene terephthalate)/Poly(ethylene isophthalate) Blends

Darwin P. R. Kint,¹ Antxon Martínez de Ilarduya,¹ A. Sansalvadó,² Josep Ferrer,² Sebastián Muñoz-Guerra¹

¹Departament d'Enginyeria Química, Universitat Politècnica de Catalunya, ETSEIB, Diagonal 647, Barcelona 08028, Spain

²Catalana de Polímers, S.L., Avda Remolar s/n, El Prat de Llobregat, Barcelona 08820, Spain

Received 23 July 2002; accepted 21 April 2003

ABSTRACT: Physical blends of poly(ethylene terephthalate) (PET) and poly(ethylene isophthalate) (PEI), abbreviated PET/PEI (80/20) blends, and of PET and a random poly(ethylene terephthalate-co-isophthalate) copolymer containing 40% ethylene isophthalate (PET₆₀I₄₀), abbreviated PET/PET₆₀I₄₀ (50/50) blends, were melt-mixed at 270°C for different reactive blending times to give a series of copolymers containing 20 mol % of ethylene isophthalic units with different degrees of randomness. ¹³C-NMR spectroscopy precisely determined the microstructure of the blends. The thermal and mechanical properties of the blends were evaluated by DSC and tensile assays, and the obtained results were compared with those obtained for PET and a statistically random PETI copolymer with the same composition. The microstructure of the blends gradually changed from a physical blend into a block copolymer, and finally into a

random copolymer with the advance of transreaction time. The melting temperature and enthalpy of the blends decreased with the progress of melt-mixing. Isothermal crystallization studies carried out on molten samples revealed the same trend for the crystallization rate. The effect of reaction time on crystallizability was more pronounced in the case of the PET/PET₆₀I₄₀ (50/50) blends. The Young's modulus of the melt-mixed blends was comparable to that of PET, whereas the maximum tensile stress decreased with respect to that of PET. All blend samples showed a noticeable brittleness. © 2003 Wiley Periodicals, Inc. *J Appl Polym Sci* 90: 3076–3086, 2003

Key words: poly(ethylene terephthalate) (PET); poly(ethylene isophthalate) (PEI); blends; block copolymers; microstructure

INTRODUCTION

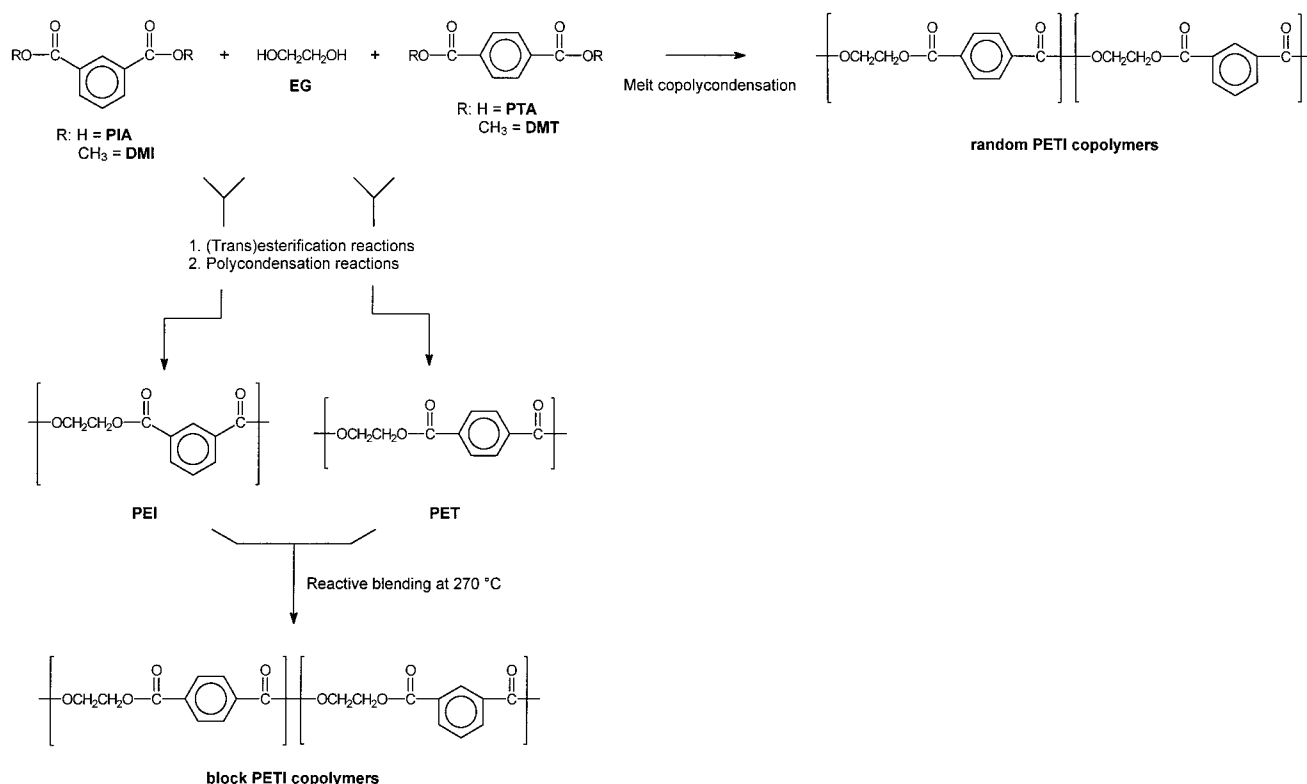
Poly(ethylene terephthalate-co-isophthalate) copolymers, abbreviated PETI, are materials of great industrial interest and extensive use. In fact, PETI copolymers containing minor amounts of ethylene isophthalic units, usually less than 10%, are currently used as thermally shrinkable packaging films, as well as heat-sealable laminating films for coating steel cans and metal and ceramic sheets. These copolymers are industrially produced by melt polycondensation reactions of mixtures of terephthalic acid (or dimethyl terephthalate), isophthalic acid (or dimethyl isophthalate), and ethylene glycol, as shown in **Scheme 1**. This copolymerization procedure leads invariably to statistically random PETIs.^{1–6} The correlation between the content in eth-

ylene isophthalic units and the crystallization behavior of random PETIs has been extensively studied.^{3–5} It is widely known that random PETIs containing 20% or more of ethylene isophthalic units are practically uncrystallizable.^{1,2}

Reactive blending of mixtures of homopolyesters is considered an advantageous course for production of industrial copolyesters without requiring significant changes in the processing equipment.^{7–17} Transreactions may proceed according to three mechanisms: alcoholysis by hydroxyl end group, acidolysis by acidic end groups, and intrachain ester exchange (transesterification).¹⁸ Transreactions convert blends first into block copolymers, finally giving random copolymers. Reactive blending of poly(ethylene terephthalate) (PET) and poly(ethylene isophthalate) (PEI) mixtures has already proved to be a successful and inexpensive route for producing block PETI copolymers with modified properties. The relationship between the microstructure and the thermal properties and crystallizability of block and random PETI copolymers was previously studied by Ha et al.¹⁹ They reported on block PETI copolymers containing 40% of ethylene isophthalate, which were obtained by reac-

Correspondence to: S. Muñoz-Guerra (sebastian.munoz@upc.es).

Contract grant sponsor: Comisión Interministerial de Ciencia y Tecnología (CICYT); contract grant numbers: MAT99-0578-CO2-02 and FD-97-1585.



Scheme 1 Schematic representation of different copolymerization procedures for preparation of homopolyesters and copolyesters (from Kint and Muñoz-Guerra¹¹).

tive blending of PET/PEI (60/40) mixtures. The copolyester microstructure was characterized by ¹H-NMR spectroscopy, using the analytical method proposed by Po' et al.^{20–22} The resolution achieved with this method, however, appeared insufficient to measure the sequence lengths and distribution with accuracy and certainty.

In this work we report on PET₈₀I₂₀ copolymers, that is, copolymers containing 20% of ethylene isophthalic units, prepared by reactive blending using two different initial mixtures: (1) PET/PEI (80/20) and (2) PET/random PET₆₀I₄₀ (50/50) mixtures. By these means not only block ethylene isophthalic sequences but also random ethylene terephthalic/ethylene isophthalic (60/40) block sequences will be introduced into the PET homopolymer. The change in microstructure with the advance of transreactions was followed by ¹³C-NMR analysis by applying a methodology previously developed by us, which is able to determine the microstructure of these copolyesters.²³ The thermal and mechanical properties, as well as the crystallizability, were evaluated for PETIs differing not only in composition but also in the fine microstructure. Comparison of these evaluation results with ¹³C-NMR data enabled us to correlate thermal properties and microstructure of PETI copolymers in a more detailed manner than attempted before.

EXPERIMENTAL

Materials

Dimethyl isophthalate (DMI; >99%) and ethylene glycol (EG; >99%) were purchased from Sigma-Aldrich Co. (St. Louis, MO). Both were commercial reagent-grade products and were used without further purification. Tetrabutyl titanate catalyst (Merck-Schuchardt, Darmstadt, Germany) was used without further purification. The solvents used for purification or characterization, such as trifluoroacetic and dichloroacetic acids, methanol, chloroform, diethyl ether, and *o*-chlorophenol, were all either technical grade or high-purity grade and used as received.

Scheme 1 includes the different routes that have been followed for the preparation of the homopolyesters and copolyesters studied in this work.

The PEI homopolymer was prepared by a two-step procedure including transesterification and subsequent polycondensation reactions. DMI (20.00 g, 0.103 mol) and EG (14.06 g, 0.227 mol) were charged to a 100-mL, three-neck, round-bottom flask equipped with a mechanical stirrer, a nitrogen inlet, and a distillation column. The transesterification reaction was carried out at 185°C under a nitrogen flow for a period of 5 h using tetrabutyl titanate as a catalyst. The subsequent polycondensation reaction was performed at

260°C under a 0.5- to 1-mbar vacuum. The polymerization was allowed to proceed isothermally at this temperature for 2 h. The resulting high viscous liquid was cooled to room temperature and atmospheric pressure was recovered with a nitrogen flow to prevent degradation. The solid mass was dissolved in chloroform and the PEI homopolymer was precipitated with cold diethyl ether, collected by filtration, and extensively washed with cold methanol and diethyl ether. The sample was dried at 60°C under reduced pressure for 72 h. The intrinsic viscosity of this polyester was 0.61 dL g⁻¹, and the number- and weight-average molecular weights, determined by gel permeation chromatography (GPC), were found to be 38,700 and 75,900 g mol⁻¹, respectively. It has been reported that the formation of cyclic oligomers could prevent the production of high molecular weight PEI.²⁴ However, ¹H-NMR analysis indicated that only a very small amount of cyclic oligomers was formed and that they were removed upon purification.

The PET homopolymer and random PETI copolymers used in this work were prepared by Catalana de Polimers, S.L. (Barcelona, Spain) by melt polycondensation reactions of mixtures of terephthalic acid (PTA), isophthalic acid (PIA), and EG. The reactions were carried out in two steps. The final temperatures for the esterification step and polycondensation reaction were adjusted at 225 and 280°C, respectively. The polycondensation step was carried out under increasing vacuum and in the presence of Sb₂O₃ as a catalyst. The copolymers were purified by dissolving them in a chloroform/trifluoroacetic acid (8/1 v/v) mixture, followed by subsequent precipitation with cold diethyl ether. The powdery solid was collected by filtration and extensively washed with cold methanol and diethyl ether. Then they were dried at 60°C for 72 h under reduced pressure.

The physical PET/PEI (80/20) and PET/PET₆₀I₄₀ (50/50) blends were prepared by dissolving the two respective polymers in a mixture of chloroform/TFA (8/1 v/v), followed by a subsequent coprecipitation in cold diethyl ether. The preparation of the physical blends was done quickly, to avoid the reaction of the end groups with TFA. All samples were dried at 60°C for 72 h under reduced pressure. The reactive blending of the physical blends was accomplished in a mixing molder (Model CS-183 MMX mini-max molder) at 270°C for specified times without the use of a catalyst. After reactive blending, the samples were stored under vacuum at room temperature. GPC measurements revealed that the molecular weight slightly decreased with the advance of the melt-mixing process. The thermal stability of the melt-mixed blends was assessed by thermogravimetric analysis and was found to remain unaltered compared to the thermal stability of PET, PEI, and the initial physical blends.

Measurements

Solution ¹H- and ¹³C-NMR spectra were recorded on a Bruker AMX-300 spectrometer (Germany) at 25.0 ± 0.1°C, operating at 300.1 and 75.5 MHz, respectively. The polyesters and blends were dissolved in deuterated trifluoroacetic acid (TFA-*d*₁), and the obtained spectra were internally referenced to tetramethylsilane. Samples (10 and 50 mg) dissolved in 1 mL of deuterated solvent were used for ¹H- and ¹³C-NMR, respectively. For ¹H-NMR spectra, 64 scans were acquired with 32K data points and a delay time of 1 s. For ¹³C-NMR spectra, the pulse and spectral widths were 4.3 μs (90°) and 18 kHz, respectively, and the relaxation delay was 2 s. From 5000 to 15,000 free induction delays were acquired with 64K data points and Fourier transformed (FT) with 128K, providing a digital resolution of 0.27 Hz per point. Integration of the overlapping signals was made by Lorentzian deconvolution of the spectra using the Bruker 1D WIN NMR computer software.

The intrinsic viscosity [η] of PET and PEI homopolymers and the random PETI copolymers was measured from dichloroacetic acid solutions with a Ubbelohde viscometer (Cannon-Ubbelohde, State College, PA) thermostated at 25 ± 0.1°C. GPC measurements were performed on a Waters GPC system (Waters Chromatography Division/Millipore, Milford, MA) equipped with a refractive index detector. The eluent was an *o*-chlorophenol/chloroform (1/9 v/v) mixture. Two 7.8 × 300-mm Styragel columns packed with divinylbenzene crosslinked polystyrene (pore size = 10³ and 10⁴ Å) in series were used for the analysis with the aforementioned eluent at a flow rate of 0.5 mL min⁻¹ at 35°C. The molecular weights and the molecular weight distributions were calculated against monodisperse polystyrene standards with the Maxima 820 software.

The thermal properties of the polyesters and the melt-mixed blends were evaluated by differential scanning calorimetry (DSC) with a Perkin-Elmer DSC Pyris 1 (Perkin Elmer Cetus Instruments, Norwalk, CT). Thermograms were obtained from 4- to 6-mg samples at heating and cooling rates of 10°C min⁻¹ under a nitrogen flow of 20 mL min⁻¹. Indium and zinc were used as standards for the temperature and enthalpy calibration. Isothermal crystallization studies were performed on molten samples at 165°C. Tensile testing was performed on rectangular specimens (55 × 5 mm) cut from amorphous, isotropic films having a thickness of about 200 μm. The tensile tests were conducted at room temperature on a Zwick (Germany) BZ2.5/TN1S universal tensile testing apparatus operating at a constant crosshead speed of 10 mm min⁻¹ using a 0.5-N preload and a grip-to-grip separation of 20 mm. All reported tensile data represent an average of at least six independent measurements.

TABLE I
Characteristics and Thermal Properties of Amorphous PET and Random PETI Copolyesters

Polyester	Composition ^a		DEG ^b	Molecular weights			Thermal properties			
	X _T	X _I		[η] ^c	M _n ^d	M _w ^d	T _g ^e	T _{cc} ^f	T _m ^f	ΔH _m ^f
PET	100	0	2.2	0.63	18,300	51,200	78	137	253	46.9
PET ₉₈ I ₂	97.6	2.4	2.3	0.69	21,100	49,600	77	138	251	36.8
PET ₉₄ I ₆	93.9	6.1	2.5	0.71	22,300	58,000	74	151	242	27.2
PET ₉₀ I ₁₀	90.1	9.9	2.4	0.65	19,700	50,900	72	159	233	24.0
PET ₈₅ I ₁₅	87.3	12.7	2.4	0.64	18,600	49,500	72	169	229	14.3
PET ₈₀ I ₂₀	82.2	17.8	2.4	0.68	19,100	47,300	71	— ^g	—	—
PET ₆₀ I ₄₀	60.2	39.8	3.3	0.70	18,900	49,100	69	—	—	—
PEI	0	100	2.3	0.61	38,700	75,900	59	147	245	1.4

^a Determined from the aromatic proton resonances observed in ¹H-NMR spectra (mol %).

^b Diethylene glycol content (mol %) calculated from ¹H-NMR spectra.

^c Intrinsic viscosity (dL g⁻¹) measured in dichloroacetic acid at 25°C.

^d Number- and weight-average molecular weights determined by GPC.

^e Glass-transition temperature (T_g; °C) taken as the inflection point of the heating DSC traces of melt-quenched samples recorded at 30°C min⁻¹.

^f Cold-crystallization (T_{cc}; °C) and melting (T_m; °C) temperatures and melting enthalpy (ΔH_m; J g⁻¹) of initially amorphous samples measured by DSC at a heating rate of 10°C min⁻¹.

^g —, indicates that no cold crystallization and melting were observed for these samples under the indicated conditions.

RESULTS AND DISCUSSION

Microstructure characterization

In a previous study we reported on the analysis of PETI copolyesters by 75.5 MHz ¹³C-NMR spectroscopy carried out in a 2% (w/v) deuterated trifluoroacetic acid solution at 25.0°C.²³ Under these conditions, splitting of the nonprotonated terephthalic and isophthalic aromatic carbon signals into four and two peaks, respectively, was observed. This information allowed us to determine with high accuracy and reliability the microstructure of the PETI copolymers, including both randomness and sequence length distribution of the ethylene terephthalate and ethylene isophthalate sequences. The PETI copolyesters obtained by melt polycondensation included copolymers with a content of ethylene isophthalic units ranging from 2 to 40%. Their characteristics are listed in Table I, together with those for the two parent homopolymers PET and PEI. The microstructure of these copolyesters was found to be at random for whichever composition.

The same methodology was applied to the analysis of PET₈₀I₂₀ samples obtained by reactive blending. Figure 1 shows the compared ¹³C-NMR spectra for the nonprotonated aromatic carbons of the terephthalic and isophthalic units for the PET/PEI (80/20) blend samples melt-mixed for the indicated times. In the spectrum of the physical polymer blend, both signals consisted of one peak, associated with the homopolymer. Upon reaction, new peaks appeared whose intensity increased as a function of the reaction time. As indicated, these new peaks are assigned to the different dyad and triad sequences formed by transesterification, with T standing for terephthalic and I for

isophthalic units, respectively. Signal assignment was accomplished as described elsewhere.²³ The IT dyad and the TTI and ITI triads increased progressively with the extent of reaction. With the relative integral values of the dyad and triad signals, the distribution of the possible types of dyads centered in I (II and IT) and triads centered in T (TTT, TTI, and ITI) could be calculated, respectively. On the basis of these data, the number-average sequence lengths of the ethylene terephthalic (n_T) and ethylene isophthalic (n_I) units, and the degree of randomness (R) could be estimated as follows:

$$n_T = \frac{N_{TTT} + \left(\frac{N_{TTI} + N_{ITI} + N_{IT} }{2} \right)}{\left(\frac{N_{TTI} + N_{ITI} + N_{IT} }{2} \right)}$$

$$n_I = \frac{N_{II} + \left(\frac{N_{TTI} + N_{ITI} + N_{IT} }{2} \right)}{\left(\frac{N_{TTI} + N_{ITI} + N_{IT} }{2} \right)}$$

$$R = \frac{1}{n_T} + \frac{1}{n_I}$$

where N_i is the molar fraction of the i type of sequences. This value is directly proportional to the integrated area under the peak associated with the

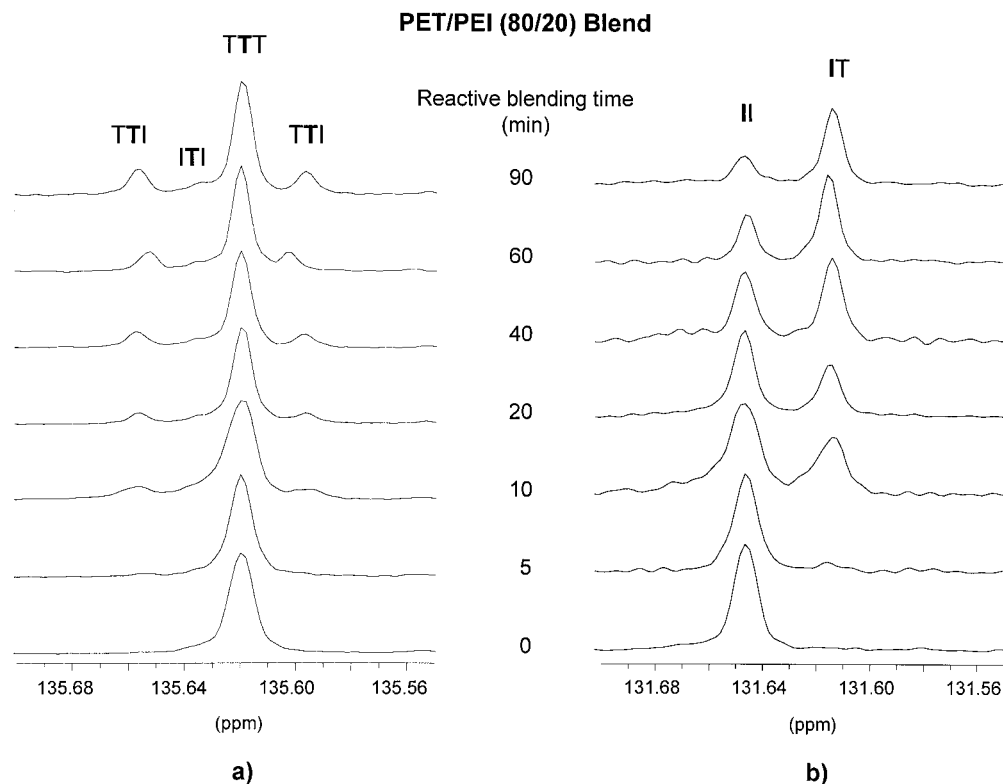


Figure 1 Evolution of the ^{13}C -NMR spectra for the nonprotonated aromatic carbons of the (a) terephthalic and (b) isophthalic units with the advance of reactive blending for the PET/PEI (80/20) blend.

sequence of interest. The obtained results are given in Table II, and the evolution of the randomness and sequence lengths with the progress of reactive blending is illustrated in Figure 2. The microstructure of the melt-mixed PET/PEI (80/20) blend was found to change from that corresponding to the initial two homopolymer mixture to an intermediate block $\text{PET}_{80}\text{I}_{20}$ copolymer, and finally to a nearly random $\text{PET}_{80}\text{I}_{20}$ copolymer.

The evolution of the ^{13}C -NMR spectra for the nonprotonated aromatic carbons of the terephthalic and isophthalic units upon reactive blending of the PET/ $\text{PET}_{60}\text{I}_{40}$ (50/50) blend is presented in Figure 3, and the resulting data are given in Table III. Figure 4 shows the change in randomness and the average sequence lengths of the ethylene terephthalate and ethylene isophthalate sequences of these blends. Because $\text{PET}_{60}\text{I}_{40}$ is a random copolymer, the initial

TABLE II
Sequence Distribution and Randomness of the Melt-Mixed PET/PEI (80/20) Blends

Blend	Reactive blending time (min)	Triad (mol %)			Dyad (mol %)		Number-average sequence lengths		Randomness R
		TTT	TTI	ITI	IT	II	n_T	n_I	
PET/PEI-0	0	79.9	—	—	—	20.1	95	0	0
PET/PEI-5	5	75.3	3.8	0.2	1.6	19.1	41.7	11.3	0.11
PET/PEI-10	10	68.4	10.9	0.5	6.5	13.7	12.0	3.2	0.40
PET/PEI-20	20	66.4	11.5	1.3	7.6	13.2	10.1	2.8	0.46
PET/PEI-40	40	62.5	15.6	1.5	10.9	9.5	7.2	1.9	0.65
PET/PEI-60	60	60.5	17.4	1.7	13.8	6.6	6.0	1.5	0.81
PET/PEI-90	90	58.4	19.2	1.9	14.2	6.3	5.5	1.5	0.85
$\text{PET}_{80}\text{I}_{20}^a$	—	56.7	21.5	2.3	14.9	4.6	5.1	1.3	0.95

^a Random copolyester containing 20 mol % ethylene isophthalate.

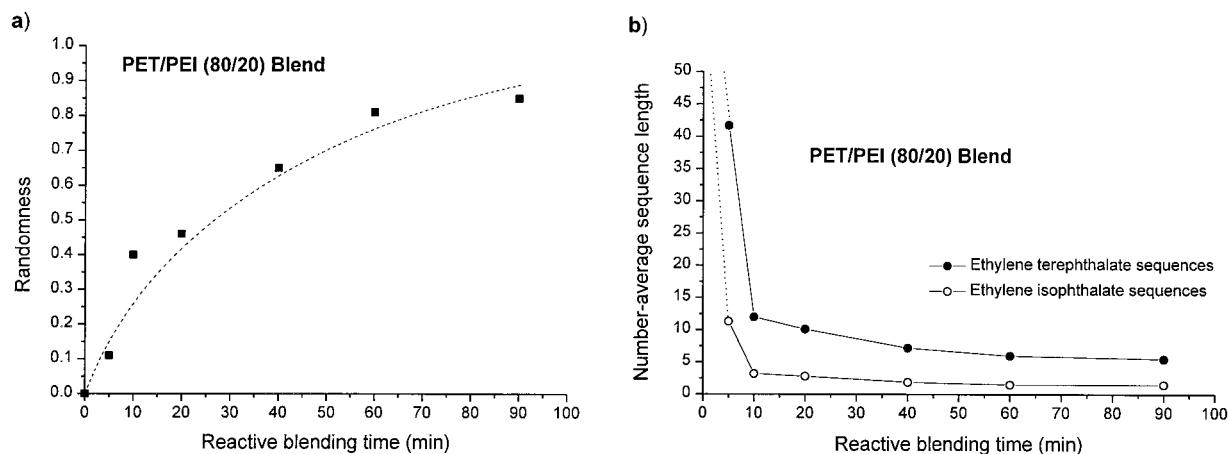


Figure 2 (a) Randomness and (b) number-average sequence lengths of the ethylene terephthalate and ethylene isophthalate sequences of melt-mixed PET/PEI (80/20) blends versus the reactive blending time.

physical PET/PET₆₀I₄₀ blend exhibited resonance peaks attributed to random sequences. Therefore, NMR analysis overestimates the number-average sequence lengths and the randomness of the melt-mixed blends, but still provided evidence that transreactions took place upon reactive blending. The PET/PET₆₀I₄₀ blend was believed to change from a physical blend into block PETI copolymers with ethylene terephthalate and random ethylene terephthalate/ethylene isophthalate blocks. These blocks became shorter and

the blend randomized with the advance of reactive blending.

Thermal analysis

The thermal properties of the random PETI copolymers prepared by melt polycondensation are compared in Table I. As expected, the glass-transition and melting temperatures and melting enthalpy of PET decreased with the incorporation of the ethylene isophthalic units.

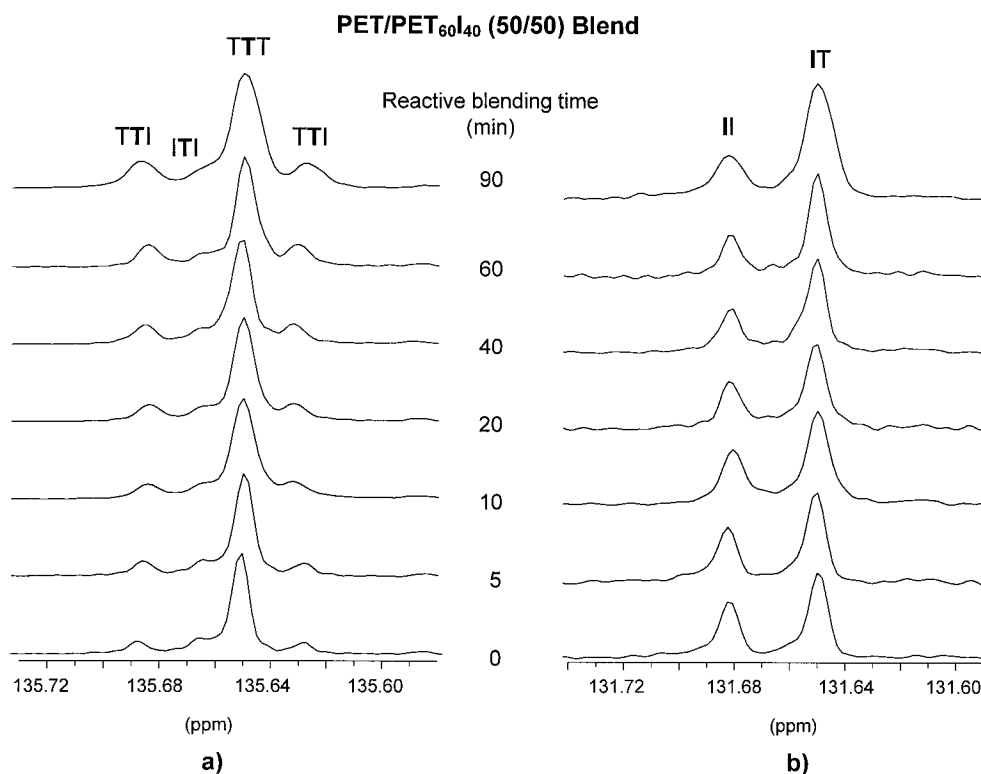


Figure 3 Evolution of the ¹³C-NMR spectra for the nonprotonated aromatic carbons of the (a) terephthalic and (b) isophthalic units with the advance of reactive blending for the PET/PET₆₀I₄₀ (50/50) blend.

TABLE III
Sequence Distribution and Randomness of the Melt-Mixed PET/PET₆₀I₄₀ (50/50) Blends

Blend	Reactive blending time (min)	Triad (mol %)			Dyad (mol %)		Number-average sequence lengths		Randomness R
		TTT	TTI	ITI	IT	II	n_T	n_I	
PET/PET ₆₀ I ₄₀ -0	0	60.2	13.2	5.6	12.2	8.8	5.9	1.7	0.75
PET/PET ₆₀ I ₄₀ -5	5	60.0	14.1	4.5	12.8	8.6	5.9	1.7	0.75
PET/PET ₆₀ I ₄₀ -10	10	59.8	15.0	3.9	13.2	8.0	5.9	1.7	0.78
PET/PET ₆₀ I ₄₀ -20	20	57.9	16.8	4.1	13.6	7.6	5.4	1.6	0.82
PET/PET ₆₀ I ₄₀ -40	40	58.1	17.4	3.5	13.9	7.0	5.5	1.5	0.83
PET/PET ₆₀ I ₄₀ -60	60	55.5	19.6	3.4	15.1	6.5	4.9	1.5	0.89
PET/PET ₆₀ I ₄₀ -90	90	54.9	20.1	3.2	15.7	6.1	4.8	1.4	0.91
PET ₆₀ I ₄₀ ^a	—	22.6	27.9	9.6	22.7	17.2	2.0	1.7	1.08

^a Random copolyester containing 40 mol % ethylene isophthalate.

Such behavior can be reasonably explained by the fact that the crystallizable PET sequences become shorter for PETIs with higher contents of ethylene isophthalate. Assuming that the isophthalic units are excluded from the crystallites, smaller and less perfect crystallites will thus result for PETIs having higher contents of ethylene isophthalate, which will be reflected in a depression of both melting temperature and enthalpy.

The thermal behavior of the melt-mixed blends was then studied and the resulting data are given in Table IV. The physical PET/PEI (80/20) blend showed a single glass-transition temperature (T_g) at 76.4°C. This transition could be assigned to the T_g of the PET phase, whereas the T_g of the PEI phase could not be detected, most probably because of the low amount of PEI. The physical PET/PEI (80/20) blend is considered to be immiscible. However, all melt-mixed PET/PEI (80/20) blends exhibited a single T_g , which was intermediate between the T_g values of PET and PEI and in accordance with the composition of the blend. This behavior is typical for a miscible blend. As the NMR results showed, the transreactions created block

copolymers, and these might act as a compatibilizer between the PET-rich and PEI-rich phases, improving the miscibility of the blends, which will result in a homogeneous mixture exhibiting a single glass-transition temperature. A single T_g value intermediate between that of PET and PET₆₀I₄₀ was found for the physical PET/PET₆₀I₄₀ (50/50) blend, indicating that this physical blend is miscible. With the advance of reactive blending the T_g value remained unchanged.

Both type of blends showed a cold-crystallization exotherm for all samples upon heating. The cold-crystallization temperature increased with the advance of reactive blending time. The melting temperature and enthalpy of the melt-mixed blends decreased with the progression of the transreactions, which is an indication that the crystallizability of the blends decreased upon reactive blending. This might suggest that crystallization was hindered because of the disruption of the chain periodicity as a consequence of the transreactions. The crystallizable ethylene terephthalate sequences were shortened with the extent of reaction, which resulted in smaller crystallites showing a lower

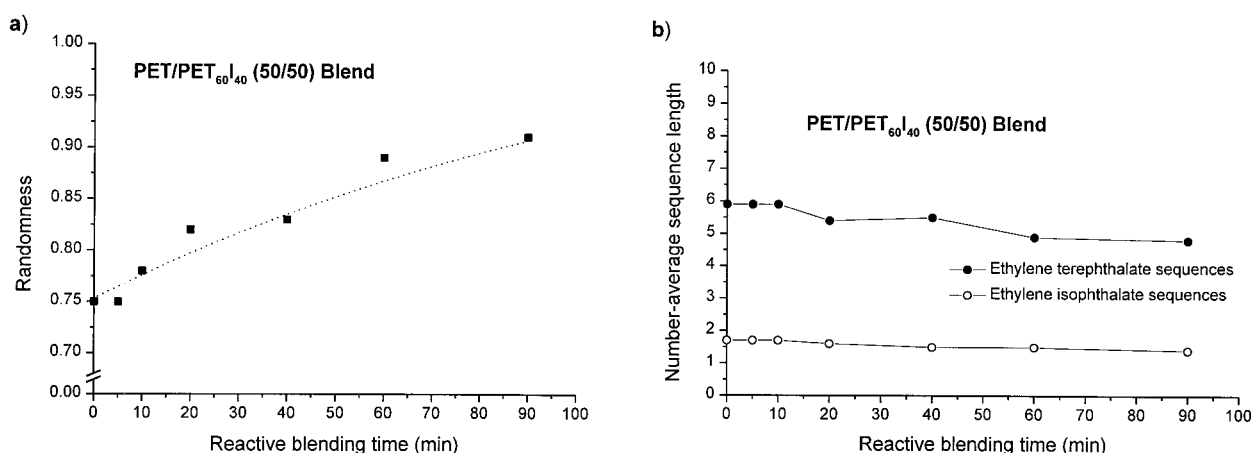


Figure 4 (a) Randomness and (b) number-average sequence lengths of the ethylene terephthalate and ethylene isophthalate sequences of melt-mixed PET/PET₆₀I₄₀ (50/50) blends versus the reactive blending time.

TABLE IV
Thermal Properties of Amorphous Melt-Mixed Blends

Blend	T_g^b	First heating ^a			Cooling ^a		Second heating ^a			
		T_{cc}	T_m	ΔH_m	T_c	ΔH_c	T_{cc}	ΔH_{cc}	T_m	ΔH_m
PET/PEI-0	76.4	138	252	35.8	149	0.6	166	-7.9	226	10.0
PET/PEI-5	71.3	137	253	38.5	150	3.5	160	-10.8	228	16.4
PET/PEI-10	70.9	140	250	42.5	154	15.1	151	-7.4	227	21.8
PET/PEI-20	70.8	148	239	26.3	— ^c	—	168	-7.0	220	7.8
PET/PEI-40	69.3	150	225	22.3	—	—	172	-5.8	213	7.2
PET/PEI-60	70.3	158	224	18.5	—	—	166	-4.7	212	6.7
PET/PEI-90	69.8	160	218	17.8	—	—	171	-3.5	214	5.4
PET/PET ₆₀ I ₄₀ -0	68.7	155	248	24.2	—	—	173	-9.3	224	8.8
PET/PET ₆₀ I ₄₀ -5	69.2	157	244	21.3	—	—	168	-11.2	223	12.2
PET/PET ₆₀ I ₄₀ -10	71.8	151	244	21.7	—	—	163	-11.0	224	12.6
PET/PET ₆₀ I ₄₀ -20	70.3	158	229	20.5	—	—	165	-8.7	218	9.5
PET/PET ₆₀ I ₄₀ -40	69.3	159	225	16.2	—	—	172	-6.9	213	7.0
PET/PET ₆₀ I ₄₀ -60	69.9	169	212	11.9	—	—	174	-3.6	211	3.4
PET/PET ₆₀ I ₄₀ -90	68.0	169	208	11.2	—	—	174	-2.8	208	3.1

^a Cold-crystallization (T_{cc} ; °C), melting (T_m ; °C), and crystallization (T_c ; °C) temperatures and their respective enthalpies (J g⁻¹) measured by DSC at a heating/cooling rate of 10°C min⁻¹.

^b Glass-transition temperature (°C) taken as the inflection point of the heating DSC traces of the amorphous samples recorded at 10°C min⁻¹.

^c —, indicates that no crystallization occurred for these samples upon cooling.

melting temperature and enthalpy. However, the PET/PEI (80/20) blends after 5 and 10 min of reactive blending showed a small increase in the melting temperature and enthalpy, compared to that of the physical blend. Furthermore, these blends could crystallize from the melt, whereas the physical blend hardly crystallized when cooled from the molten state at 10°C min⁻¹. These results might be an indication that these melt-mixed blends crystallize faster than the physical blends.

Isothermal crystallization studies

To study in more detail the crystallization behavior and rate of the melt-mixed blends, isothermal crystallization studies were conducted on molten samples of PET, random PETI copolyesters, and the melt-mixed blends at 165°C. The kinetics of the isothermal crystallization rate is commonly determined by the Avrami relation²⁵:

$$1 - X_t = \exp[-k(t - t_0)^n] \quad (1)$$

where X_t is the relative weight fraction of crystallinity developed in the crystallization time t , t_0 is the onset crystallization time, k is the growth rate constant, and n is the Avrami exponent reflecting the nucleation mechanism and growing dimensionality. When X_t for PET and the random PETI samples is plotted against the elapsed crystallization time, typical sigmoidal-

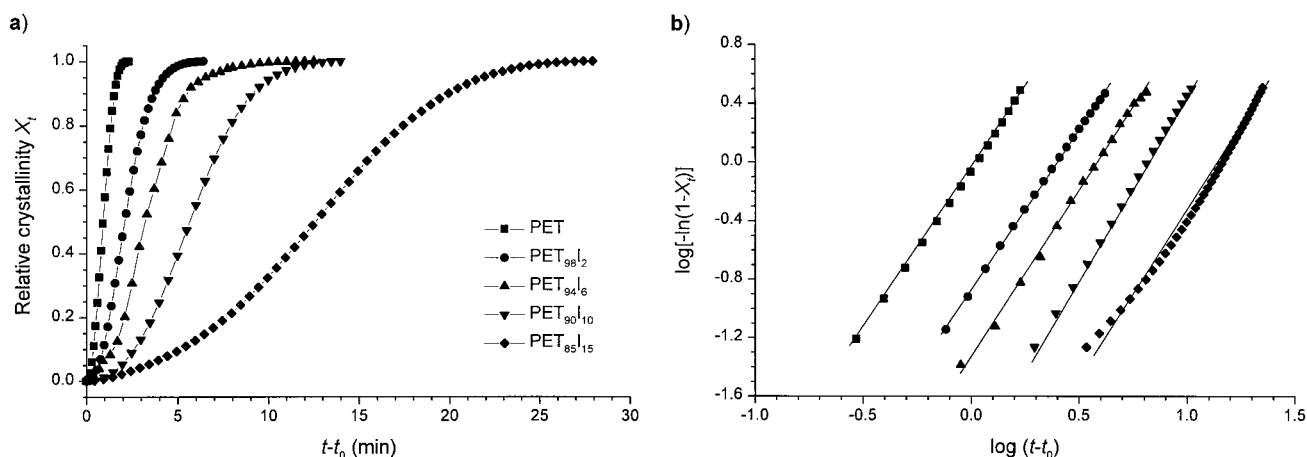


Figure 5 (a) Relative crystallinity X_t versus crystallization time and (b) Avrami plots for PET and random PETI copolymers isothermally crystallized from the melt at 165°C.

TABLE V
Crystallization Parameters of the Isothermally Crystallized Random PETI Copolyesters and Melt-Mixed Blends

	t_0^b	Avrami parameters ^a		
		n	$\log k$	$t_{1/2}$
Polyester				
PET	0.40	2.2	-0.05	0.89
PET ₉₈ I ₂	0.44	2.2	-0.87	2.11
PET ₉₄ I ₆	0.51	2.3	-1.33	3.28
PET ₉₀ I ₁₀	0.54	2.5	-2.01	5.62
PET ₈₅ I ₁₅	0.58	2.2	-2.59	12.11
PET ₈₀ I ₂₀		unable to crystallize		
Blend				
PET/PEI-0	0.37	2.2	-0.30	1.16
PET/PEI-10	0.34	2.3	0.44	0.55
PET/PEI-20	0.48	2.5	-1.20	2.62
PET/PEI-40	0.52	2.7	-1.76	3.97
PET/PEI-60	0.54	2.7	-2.23	5.73
PET/PEI-90	0.97	2.6	-2.30	6.64
PET/PET ₆₀ I ₄₀ -0	0.37	2.1	-1.56	4.59
PET/PET ₆₀ I ₄₀ -10	0.44	2.1	-1.57	4.67
PET/PET ₆₀ I ₄₀ -20	0.51	2.6	-2.00	5.06
PET/PET ₆₀ I ₄₀ -40	0.54	2.9	-2.66	7.09
PET/PET ₆₀ I ₄₀ -60	0.54	2.4	-2.61	10.91
PET/PET ₆₀ I ₄₀ -90		unable to crystallize		

^a Avrami exponent n , constant of crystallization k (min^{-1}), and crystallization half-time $t_{1/2}$ (min).

^b Onset crystallization time (min).

shaped crystallization isotherms are obtained, as illustrated in Figure 5(a). The double-logarithmic representation of eq. (1) for the isothermally crystallized samples affords the typical Avrami plots, which are compared in Figure 5(b). The value of n is obtained from the slope of these straight lines within the primary crystallization area, whereas the intercept at $\log(t - t_0) = 0$ yields the k value. The obtained crystallization parameters n and k are given in Table V. It is observed that the Avrami exponent ranged from 2.2

to 2.5, which indicates that the crystallization of PET and the random PETI samples was most likely initiated by a heterogeneous nucleation and proceeded by a three-dimensional spherulitic growth. It was observed that t_0 , k , and the crystallization half-time $t_{1/2}$ increased with the content in ethylene isophthalic units, indicating that these units had a depressing effect on the crystallization rate of PET. Random PET₈₀I₂₀ was unable to crystallize from the melt at 165°C.

Figure 6(a) shows the evolution of the relative crystallinity versus the crystallization time for the melt-mixed PET/PEI (80/20) blends, and the Avrami plots obtained for these samples are presented in Figure 6(b). The general trend is that the crystallization rate decreased with the time of treatment, PET/PEI-10 being the exceptional case, whereas the Avrami exponent remained essentially unchanged. For some samples, deviation of the straight Avrami plots could be observed, most likely because of the occurrence of secondary crystallization, which is known to start after spherulite impingement and to take place in the interlamellar regions at a much lower rate than primary crystallization.

The change in X_t with the progress of isothermal crystallization for the melt-mixed PET/PET₆₀I₄₀ (50/50) blends is shown in Figure 7(a). The resulting Avrami plots are given in Figure 7(b), and the Avrami parameters derived from these plots are listed in Table V. It was observed that the physical and all melt-mixed blends crystallized with the same mechanism as PET, although at a much slower rate. Furthermore, with the advance of reactive blending, the crystallization rate decreased. Compared with the melt-mixed PET/PEI (80/20) blends being reactively blended for the same period of time, the crystallization rate was lower for the melt-mixed PET/PET₆₀I₄₀ (50/50) blends.

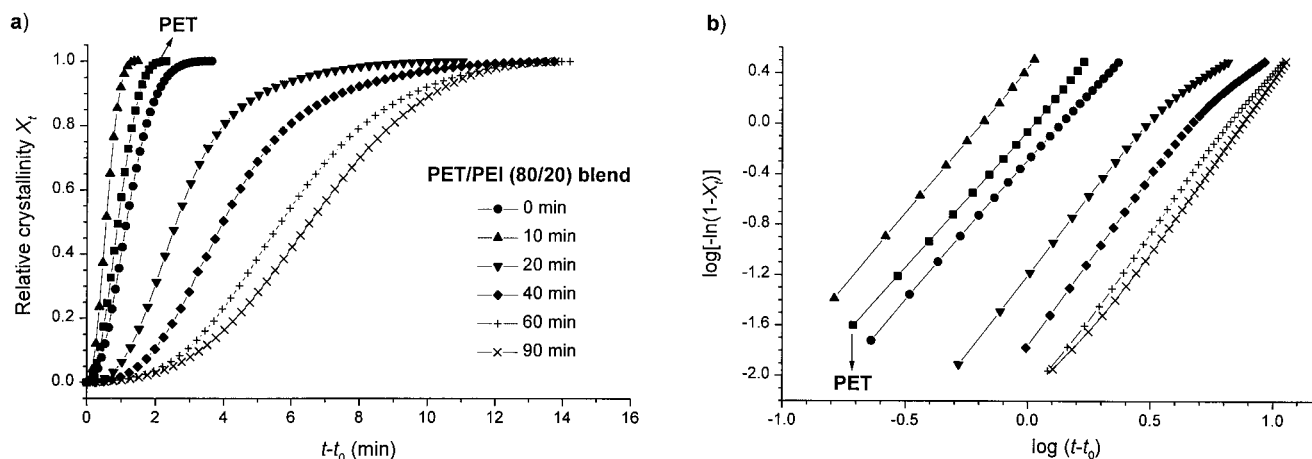


Figure 6 (a) Relative crystallinity X_t versus crystallization time and (b) Avrami plots for the melt-mixed PET/PEI (80/20) blends isothermally crystallized from the melt at 165°C.

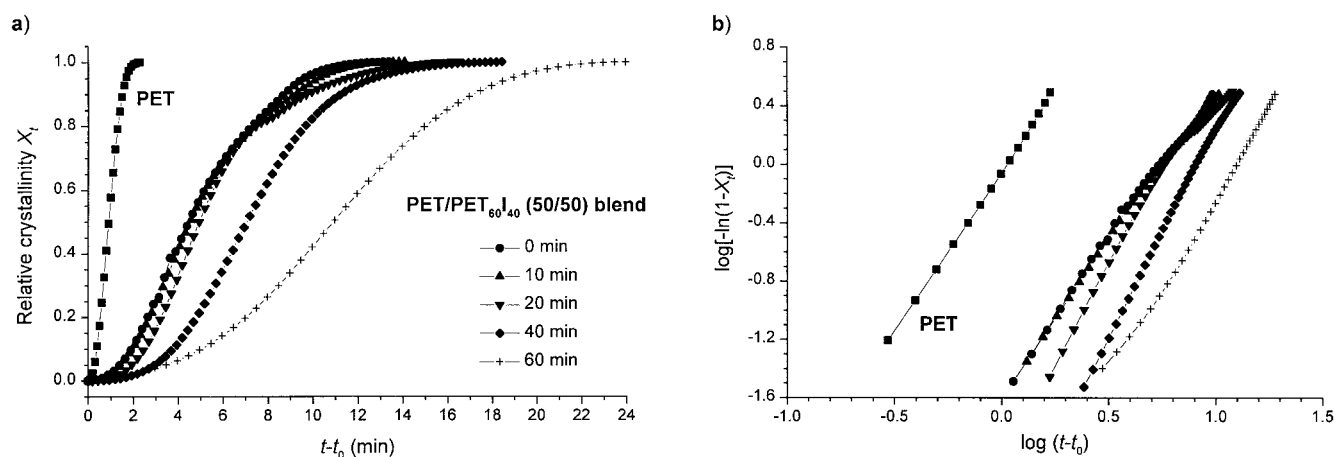


Figure 7 (a) Relative crystallinity X_t versus crystallization time and (b) Avrami plots for the melt-mixed PET/PET₆₀I₄₀ (50/50) blends isothermally crystallized from the melt at 165°C.

Tensile properties

The mechanical properties, such as the Young's modulus E , the maximum tensile stress σ_{\max} , and the elongation at break ϵ_{break} , were evaluated in tensile essays for amorphous, non-oriented PET, random PET₈₀I₂₀, and a selection of melt-mixed blends, and the results are listed in Table VI. It was observed that the PET/PEI (80/20) samples after short times of reactive blending showed very poor tensile properties, most probably attributable to the immiscible nature of these blends. With the advance of transreactions, the mechanical parameters improved and the E modulus reached a value near to that of PET and the random PET₈₀I₂₀ copolymer. However, the σ_{\max} remained significantly lower than that of PET, and all samples were highly brittle. On the other hand, miscible PET/PET₆₀I₄₀ blends showed fairly good mechanical properties, even after short reactive blending times. However, the modulus of the PET/PET₆₀I₄₀-40 sample could not be determined because this sample showed exceptionally poor tensile properties. This behavior is likely a consequence of the lower molecular weight of

the sample, which results from degradation taking place during the reactive blending treatment.

CONCLUSIONS

Transreactions took place in the physical PET/PEI (80/20) and PET/PET₆₀I₄₀ (50/50) blends, when melt-mixed at 270°C without the use of a catalyst, which was confirmed by ¹³C-NMR analysis. Triad and dyad sequences could be determined using the signals arising from the nonprotonated carbons of the terephthalic and isophthalic units, respectively, of the reacted blends. As the melt-mixing time advanced, the number-average sequence lengths decreased with a concomitant increase in the degree of randomness. For the initially immiscible PET/PEI (80/20) blend, the initial microstructure evolved from the initial physical mixture to a block copolymer, which then gradually changed into a random copolymer. A similar evolution was observed in the reactive blending of PET/PET₆₀I₄₀ (50/50), although this mixture appeared to be initially miscible. In both cases a single-phase system showing a single T_g intermediate to that of PET and PEI was obtained after 5 min of reactive blending. The "crystallizability" of PET₈₀I₂₀ copolymers, evaluated by the crystallization rate and crystallinity, was found to decrease with the transreaction time, the effect of which was more pronounced in the case of the PET/PET₆₀I₄₀ (50/50) blend. The Young's modulus of the melt-mixed blends was comparable to that of PET, whereas the maximum tensile stress decreased with respect to that of PET. All blend samples showed a noticeable brittleness.

TABLE VI
Tensile Properties of Amorphous Melt-Mixed Blends^a

Blend	Young's modulus, E (MPa)	Maximum tensile stress, σ_{\max} (MPa)	Elongation at break, ϵ_{break} (%)
PET	1440 (165)	37 (5)	82 (28)
PET ₈₀ I ₂₀	1345 (105)	42 (6)	4 (1)
PET/PEI-10	n.d.	5 (1)	<1 (0)
PET/PEI-20	1575 (135)	17 (9)	1 (1)
PET/PEI-40	1695 (180)	19 (8)	1 (0)
PET/PET ₆₀ I ₄₀ -10	1495 (95)	15 (5)	3 (3)
PET/PET ₆₀ I ₄₀ -20	1510 (110)	15 (6)	1 (1)
PET/PET ₆₀ I ₄₀ -40	n.d.	2 (1)	1 (1)

^a Standard deviations are given in parentheses. n.d. could not be precisely determined because of the poor mechanical properties.

Financial support for this work was received from the Comisión Interministerial de Ciencia y Tecnología (CICYT) (MAT99-0578-CO2-02 and FD-97-1585). The authors thank Dr. X. Vidal for assistance with the DSC experiments and Gabriela Molina for some mechanical property measure-

ments. The assistance and kind support of Dr. M. J. Fernández-Berridi (Polymer Science and Technology Department, University of the Basque Country) with the use of the MMX mini-max molding machine is gratefully acknowledged.

References

1. Lee, S. W.; Ree, M.; Park, C. E.; Jung, Y. K.; Park, C. S.; Jin, Y. S.; Bae, D. C. *Polymer* 1999, 40, 7137.
2. Li, B.; Yu, J.; Lee, S.; Ree, M. *Eur Polym J* 1999, 35, 1607.
3. Yu, J.; Li, B.; Lee, S.; Ree, M. *J Appl Polym Sci* 1999, 73, 1191.
4. Wu, T. M.; Chang, C. C.; Yu, T. L. *J Polym Sci Part B: Polym Phys* 2000, 38, 2515.
5. Li, B.; Yu, J.; Lee, S.; Ree, M. *Polymer* 1999, 40, 5371.
6. Zhang, Y.; Gu, L. *Eur Polym J* 2000, 36, 759.
7. Denchev, Z.; Duchesne, A.; Stamm, M.; Fakirov, S. *J Appl Polym Sci* 1998, 68, 429.
8. (a) Fiorini, M.; Pilati, F.; Berti, C.; Toselli, M.; Ignatov, V. *Polymer* 1997, 38, 413; (b) Ignatov, V. N.; Carraro, C.; Tartari, V.; Pippa, R.; Pilati, F.; Berti, C.; Toselli, M.; Fiorini, M. *Polymer* 1996, 37, 5883; (c) Ignatov, V. N.; Carraro, C.; Tartari, V.; Pippa, R.; Scapin, M.; Pilati, F.; Berti, C.; Toselli, M.; Fiorini, M. *Polymer* 1997, 38, 195; (d) *ibid.* 1997, 38, 201.
9. (a) Godard, P.; Dekoninck, J. M.; Devlesaver, V.; Devaux, J. *J Polym Sci Part A: Polym Chem* 1986, 24, 3301; (b) *ibid.* 1986, 24, 3315.
10. Jun, H. W.; Chae, S. H.; Park, S. S.; Myung, H. S.; Im, S. S. *Polymer* 1999, 40, 1473.
11. (a) Kint, D.; Muñoz-Guerra, S. *Polym Int* 1999, 48, 346; (b) *ibid.* 2003, 52, 321.
12. Kollodge, J. S.; Porter, R. S. *Macromolecules* 1995, 28, 4089; (b) *ibid.* 1995, 28, 4097; (c) *ibid.* 1995, 28, 4106; (d) Porter, R. S.; Wang, L. H. *Polymer* 1992, 33, 2019.
13. (a) Lee, S. C.; Yoon, K. H.; Park, I. H.; Kim, H. C.; Son, T. W. *Polymer* 1997, 38, 4831; (b) Yoon, K. H.; Lee, S. C.; Park, I. H.; Lee, H. M.; Park, O. O.; Son, T. W. *Polymer* 1997, 38, 6079.
14. (a) MacDonald, W. A.; McLenaghan, A. D. W.; McLean, G.; Richards, R. W.; King, S. M. *Macromolecules* 1991, 24, 6164; (b) Backson, S. C. E.; Kenwright, A. M.; Richards, R. W. *Polymer* 1995, 36, 1991; (c) Kenwright, A. M.; Peace, S. K.; Richards, R. W.; Bunn, A.; MacDonald, W. A. *Polymer* 1999, 40, 5851; (d) Collins, S.; Kenwright, A. M.; Pawson, C.; Peace, S. K.; Richards, R. W.; MacDonald, W. A.; Mills, P. *Macromolecules* 2000, 33, 2974.
15. Patcheak, T. D.; Jabarin, S. A. *Polymer* 2001, 42, 8975.
16. Stewart, M. E.; Cox, A. J.; Naylor, D. M. *Polymer* 1993, 34, 4060.
17. Litmanovich, A. D.; Platé, N. A.; Kudryavtsev, Y. V. *Prog Polym Sci* 2002, 27, 915.
18. Kotliar, A. M. *J Polym Sci Macromol Rev Ed* 1981, 16, 367.
19. Ha, W. S.; Chun, Y. K.; Jang, S. S.; Rhee, D. M.; Park, C. R. *J Polym Sci Part B: Polym Phys* 1997, 35, 309.
20. Po', R.; Cioni, P.; Abis, L.; Occhiello, E.; Garbassi, F. *Polym Commun* 1991, 32, 208.
21. Abis, L.; Po', R.; Bacchilega, G.; Occhiello, E.; Garbassi, F. *Makromol Chem* 1992, 193, 1859.
22. (a) Spera, S.; Po', R.; Abis, L. *Polymer* 1993, 34, 3380; (b) *ibid.* 1996, 37, 729.
23. Martínez de Ilarduya, A.; Kint, D. P. R.; Muñoz-Guerra, S. *Macromolecules* 2000, 33, 4596.
24. Berr, C. E. *J Polym Sci* 1955, 15, 591.
25. (a) Avrami, M. *J Chem Phys* 1939, 7, 1103; (b) *ibid.* 1940, 8, 212; (c) *ibid.* 1941, 9, 177.